EVALUATION OF FRACTURE TOUGHNESS, CONSTRAINT AND SIZE EFFECTS FROM CRITICAL CRACK TIP OPENING MEASUREMENTS USING CONFOCAL MICROSCOPY AND FRACTURE RECONSTRUCTION METHODS —G. R. Odette, G. E. Lucas , K. Edsinger, E. Donahue and H. Rathbun (University of California, Santa Barbara)

SUMMARY

This work demonstrates the use of confocal microscopy and fracture reconstruction methods to measure the critical crack tip opening displacement for several candidate fusion reactor structural materials — including both tempered martensitic steels and V-4Cr-4Ti — as well as other alloys for a variety of testing conditions and specimen sizes and configurations. Extensions of the method to regimes that deviate from small scale yielding, including stable crack growth and small specimens, based on local measures of toughness combined with simulations of crack tip fields, are also described.

PROGRESS AND STATUS

Introduction

Design and operation of fusion reactors will require accurate and conservative predictions of loading conditions which might result in rapid and catastrophic fracture by the unstable propagation of cracks presumed to exist in any large, complex structure. The critical crack tip opening displacement (δ^*) represents a material's fracture toughness in a way that is fully equivalent to more frequently cited measures like J_{IC}. Based on standard assumptions of elastic-plastic fracture mechanics (EPFM) and in combination with an appropriate constitutive law, δ^* can be used to evaluate the remote loads (stresses) and displacements (strains) leading to fracture initiation in cracked specimens or structures. Further, since δ^* represents a permanent record on the fracture surface, it is highly robust and can be used for conditions where conventional methods are difficult or impossible to apply, viz., dynamic loading rates; thin specimens with limited length of crack front under plane strain; wedge loading; complex (e.g. three dimensional) crack configurations; and subcritical crack growth. However, δ^* is not frequently used because it is difficult and tedious to measure. These limitations are avoided using a new method based on confocal microscopy fracture reconstruction (CM/FR). This paper demonstrates the use of confocal microscopy and fracture reconstruction methods to measure the critical crack tip opening displacement for several candidate fusion reactor structural materials as well as other alloys for a variety of testing conditions and specimen sizes and configurations.

Confocal Microscopy and Fracture Reconstruction

Kobayashi and co-workers have pioneered the development of fracture reconstruction using topographic maps of conjugate fracture surfaces to reconstruct the sequence of events involved in the fracture process [1-4]. We have further developed the fracture reconstruction method using confocal microscopy (CM) to obtain the topographic maps of fracture surfaces and a set of algorithms to construct, align and analyze conjugate fracture surfaces. These methods are described in more detail elsewhere [5,6], but are reviewed here.

The confocal microscope effectively, optically sections a surface by using a depth of focus which is small relative to the height variation of the surface features; hence, the surface is illuminated

only at the points where the focal plane intersects the fracture surface. By systematically changing the specimen position in z for a fixed focal length, a series of illumination patterns is obtained as a function of z, and these images can be recorded digitally and used to computationally reconstruct a quantitative, three-dimensional, digital image of the surface.

With conjugate topographs, it is possible to approximately reconstruct the sequence of events leading up to fracture. Conjugate fracture surfaces are matched and computationally overlapped until the position of the pre-crack is accurately represented; the surfaces are then computationally separated by an amount δ corresponding to the crack tip opening displacement. Since the reconstruction is computational, the process can be viewed from any direction, and regions of material separation represent damage evolution.

Fracture reconstruction data can be represented in a variety of ways, and several examples are illustrated in Figure 1 for ductile crack growth in an edge-cracked specimen of HT-9, a tempered martensitic stainless steel, loaded in three point bending at 20°C. Figure 1a shows both a side and top view of material separation of a crack advancing by stable, ductile fracture taken at a specific δ (= 225 μm). Intact material is represented in white, and separation in black. The top view shows damage nucleation ahead of the crack, and the side view shows the relationship between the two fracture surfaces along a specific plane perpendicular to the fracture surface and the crack front (approximately at the center of the figure above). Figure 1b shows the degree of overlap between the upper and lower fracture surfaces for a given δ (= 0 μm) as a function of position ahead of the crack tip. The upper figure illustrates this from a top view, where overlap is represented by gray scales (increasing white corresponds to increasing overlap). The lower figure represents the degree of overlap (vertical) ahead of the pre-crack tip (horizontal) averaged over the length of the crack front. As such, the lower figure can also be interpreted as the degree of crack tip opening δ_{remote} (vertical) as a function of crack advance Δa (horizontal), and thus directly corresponds to J vs Δa. Finally, a sequence of top views onto a crack plane for a series of increasing δ's is shown in Figure 1c. These images are useful for observing the sequence of events in crack initiation and growth, as well as for detecting the critical value, δ^*, at which initiation occurs. This can be used to estimate fracture toughness from [5]

$$K_{J\delta} \sim \sqrt{J_{I\delta}E'} \sim \sqrt{m\delta^* \sigma_y E'} \qquad (1)$$

where σ_y is the yield stress, and m is a factor that depends on the alloy stress-strain or constitutive properties and the specimen/structure-crack configuration. For deep cracks in bending and typical strain hardening rates, m is approximately equal to 2.

Finally, the observations of damage evolution and crack initiation can be combined with finite element analysis (FEA) of crack tip stress and strain fields to develop micromechanical models of fracture and quantify local fracture parameters.

Examples

Quasi-cleavage

Figure 2 illustrates a CM/FR sequence for fracture in an F-82H specimen (W=10mm, a/W=0.5) tested in three point bend at -73°C. Damage in the form of microcleavage cracks begins to form at a δ of about 62μm. These microcleavage cracks ultimately coalesce into a process zone crack

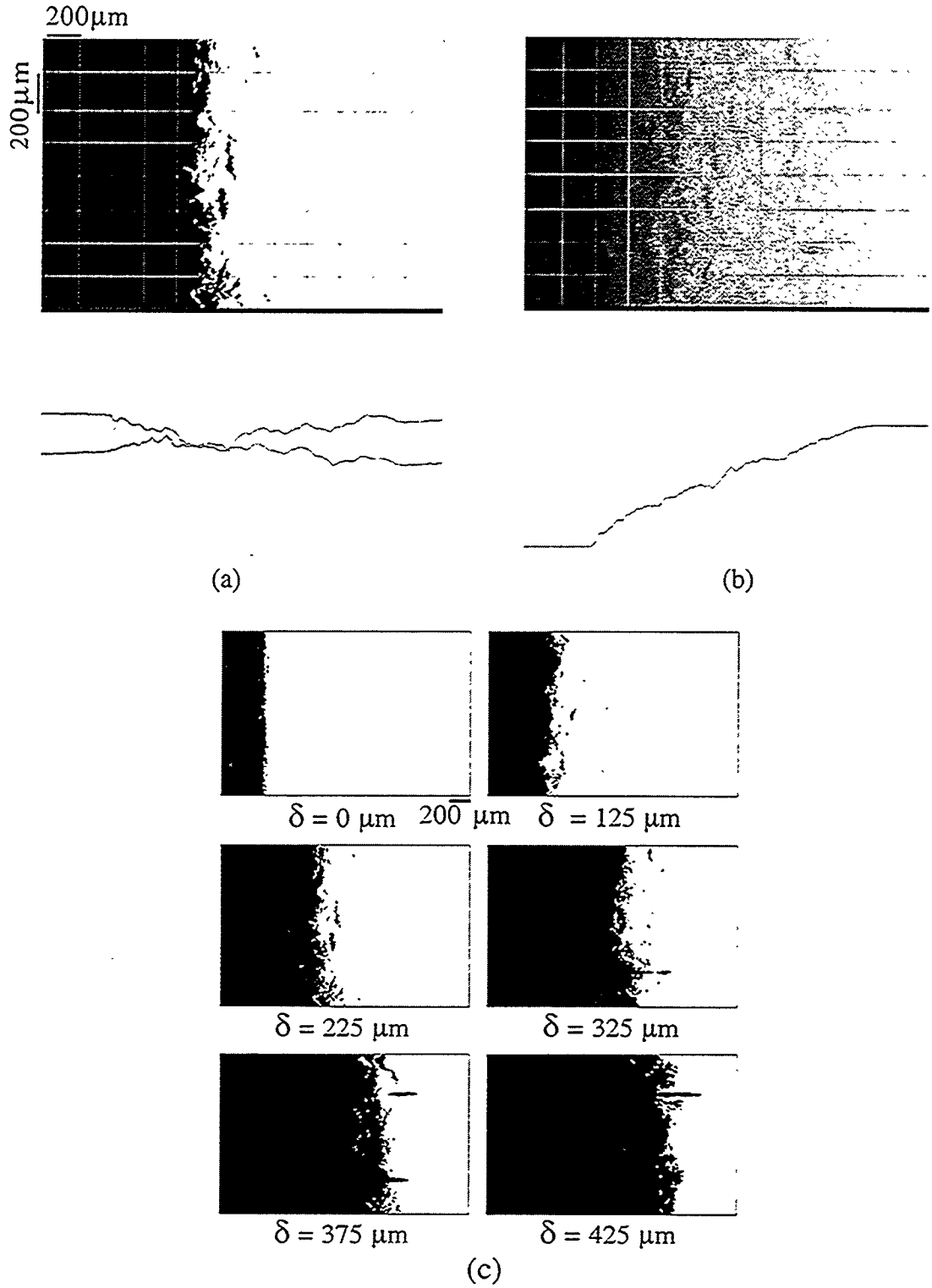

Figure 1. Illustration of the several representations of CM/FR data for HT-9: a) fracture surface separations at a fixed δ; b) conjugate fracture surface overlap at a fixed δ; c) fracture surface separations at a sequence of δ's.

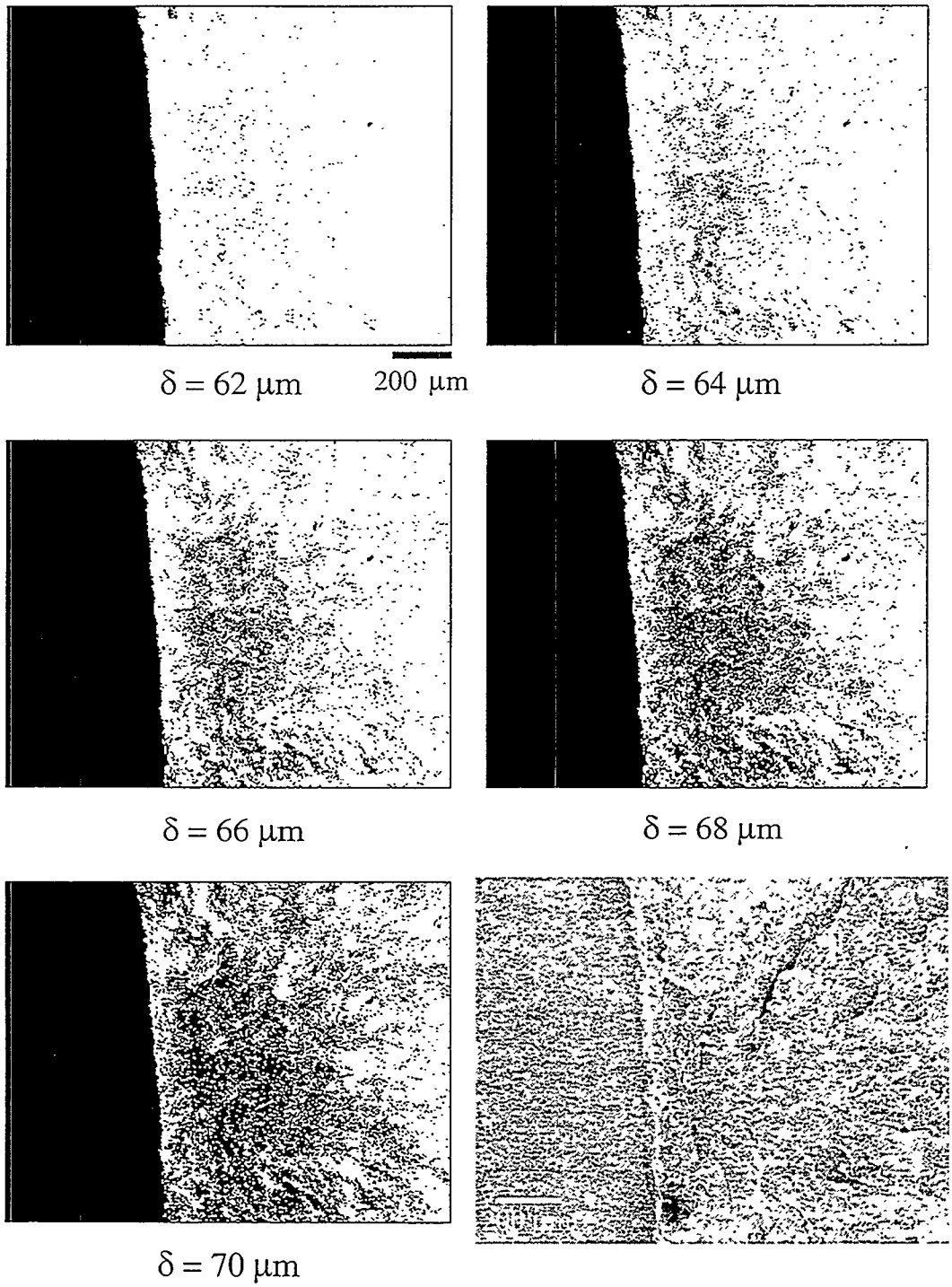

Figure 2. CM/FR sequence for fracture in an F-82H specimen (W=10mm, a/W=0.5) tested in three point bend at -73°C

that propagates unstably beyond a δ^* of 70μm. Corresponding FEA shows the initial peak damage region corresponds with peak stresses ahead of the crack tip. Similar observations and related analyses have been used to develop a micromechanical model for quasi-cleavage (and cleavage) fracture based on crack tip stresses exceeding a critical value σ^* over a critical area A^* ahead of the crack tip. [7]

Ductile Fracture

Figure 3a illustrates a CM/FR sequence for fracture in a low-alloy steel tested in three point bend at 20°C. Here, damage in the form of microvoid nucleation and growth initiates ahead of the crack tip and coalesces with the crack tip in a stable, subcritical crack growth process. The variation of δ_{remote} with Δa shown in Figure 3b closely corresponds to the mechanical J-Δa curve determined for this test and shown in Figure 3c. The minima/arrests, respectively, in these curves correspond to damage coalescence with the crack tip. The location of damage initiation observed by CM/FR can be used with high resolution scanning electron microscopy (SEM) to examine the surface for microstructural features that may play a role in crack initiation; in the case of the specimen shown in Figure 3, SEM identified a number of large particles in the damage initiation region. [5]

Fracture Toughness

Figure 4 illustrates that measures of $K_{J\delta}$ determined from CM/FR are in good agreement with values of fracture toughness, K_{Jc}, determined from analysis of mechanical load-displacement data for a wide range of alloys, specimen sizes and test conditions. Hence, CM/FR provides an opportunity to measure fracture toughness under conditions where standard techniques may not be easily applied (dynamic loading, small specimens, part through cracks, etc.)

Size Effects

All measures of toughness respond to size and geometry effects. Small or shallow cracked specimens have a higher toughness and hence higher δ^*. This is illustrated in Figure 5, where δ_{remote} vs x (distance ahead of the crack) data are plotted for pre-cracked Charpy specimens (PCC) from a low alloy steel tested at -40°C; as seen the specimen containing the shallow crack (i.e., crack length to specimen width ratio a/W=0.1) blunts to a larger δ before the onset of unstable fracture than the deeply cracked specimen (a/W=0.5). These size effects (as well as effects of irradiation and strain rate) can be modeled using the critical stress/area criteria described above in conjunction with stress fields calculated by FEA for geometries of interest. This is illustrated in Figure 6, where both pre-cracked Charpy and pre-cracked 1/3-sized-Charpy (MPCC) data on F-82H are fit by the same σ^*/A^* criteria on the lower shelf and knee, where quasi-cleavage initiation predominates .

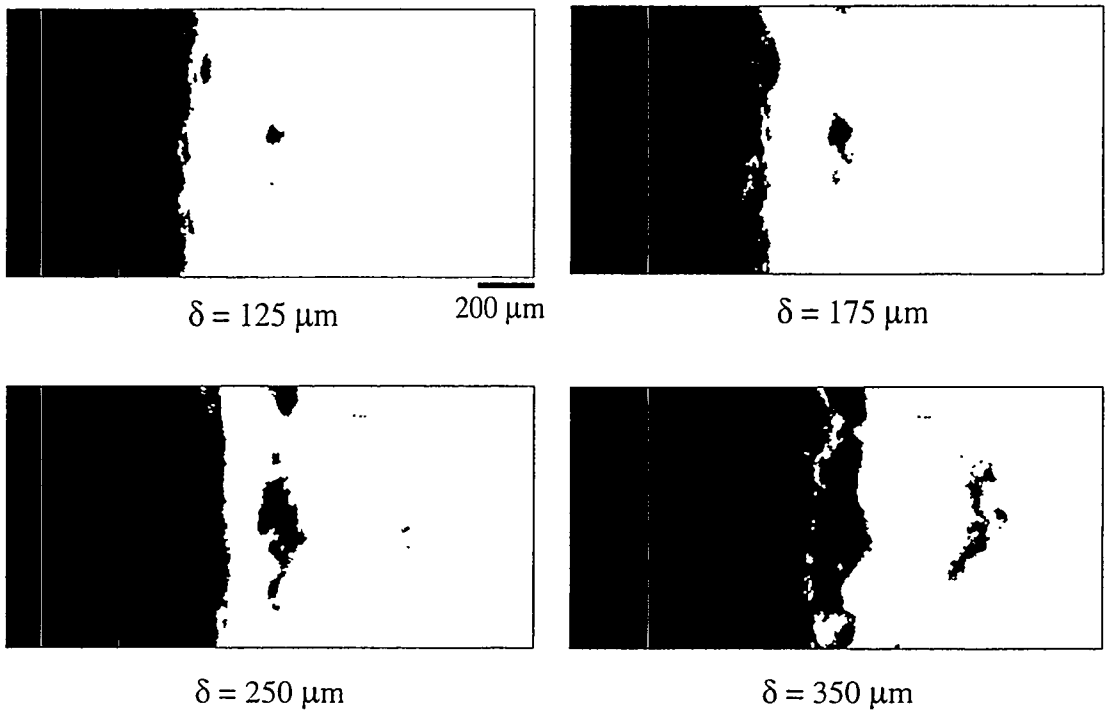

(a)

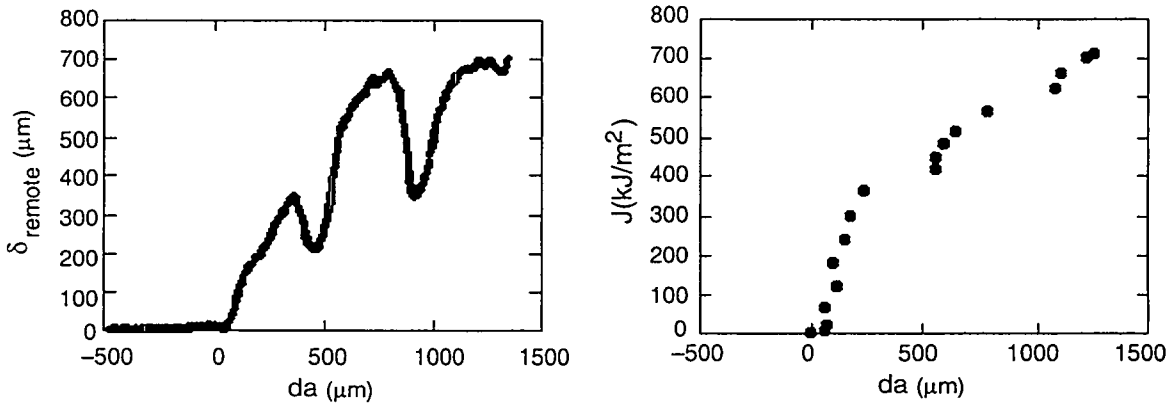

(b)

Figure 3. a) a CM/FR sequence; b) the variation of δ_{remote} with Δa; and c) mechanical J-Δa curve determined for a low-alloy steel tested in three point bend at 20°C

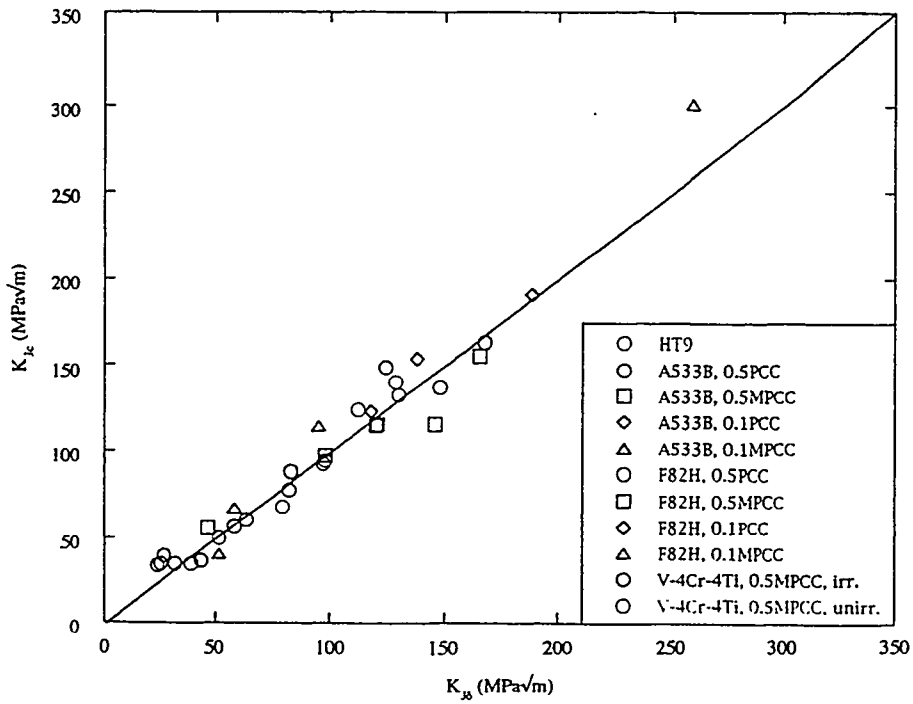

Figure 4. Comparison of $K_{\delta c}$ determined from CM/FR with K_{Jc} determined from analysis of mechanical load-displacement data for a range of alloys, test conditions and specimen sizes, including pre-cracked Charpy (PCC) and 1/3-sized Charpy (MPCC) specimens with crack length to specimen width ratios of 0.1 and 0.5.

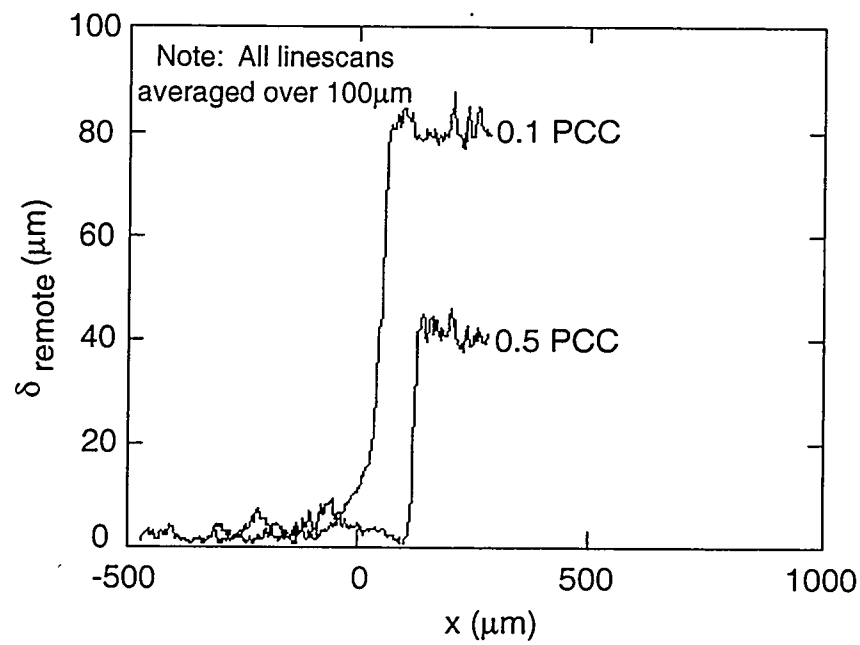

Figure 5. δ_{remote} vs x for pre-cracked Charpy specimens from a low alloy steel tested at -40°C

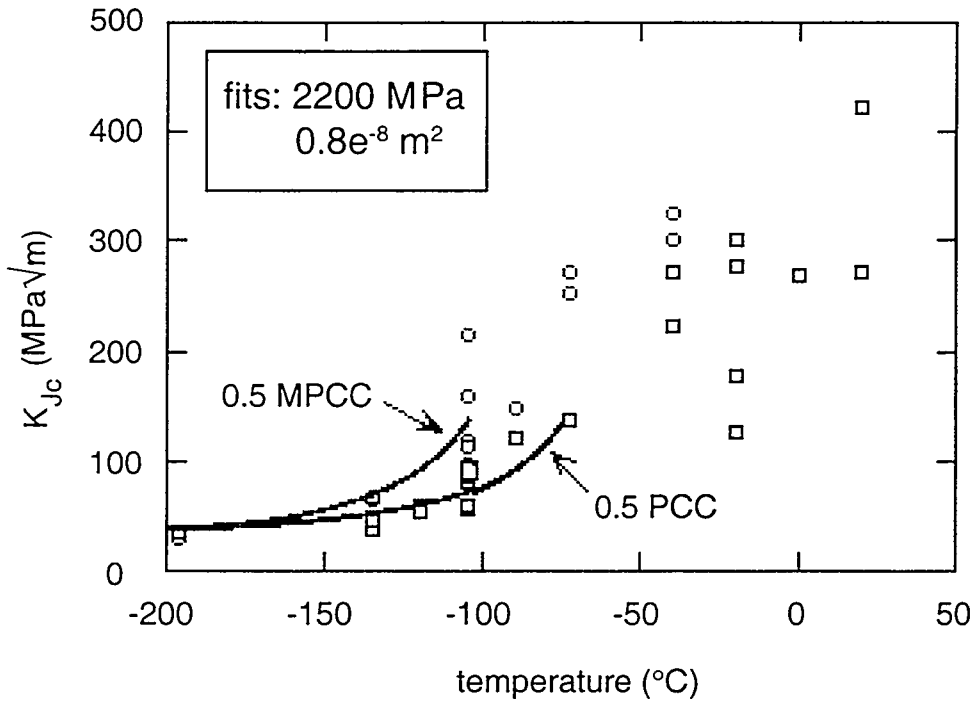

Figure 6. Effective toughness versus temperature for both pre-cracked Charpy and 1/3-sized-Charpy data in F-82H. Lines represent predictions of σ^*/A^* model.

SUMMARY AND CONCLUSIONS

The use of confocal microscopy and fracture reconstruction to observe the sequence of events in the fracture process and to measure the evolution of the crack tip opening displacement δ has been demonstrated for a variety of alloys. Values of δ^* at the point of crack initiation can be used to obtain measures of fracture toughness for a large variety of specimens and test conditions. The evolution of δ provides insight into the mechanisms of fracture; and measures of δ^* can be combined with finite element analyses of crack tip stress and strain fields to provide direct measures of local fracture parameters.

Knowledge of fracture micromechanics, quantification of local fracture parameters, and FEA can be combined to predict fracture under a variety of specimen/structure sizes/geometries and test/service conditions.

ACKNOWLEDGMENTS

This work was supported in part by the Office of Fusion Energy, DOE, Grant No. DE-FG03-87ER-52143 and the US Nuclear Regulatory Commission under contract number NRC-04-94-049.

REFERENCES

1. Ogawa, K., Zhang, X. J., Kobayashi, T., Armstrong, R. W., Irwin, G. R., ASTM-STP-833 American Society for Testing and Materials (1984) p. 393.
2. Kobayashi, T. and Shockey, D. A., Metallurgical Transactions., Vol. 18A (1987) p. 1941.
3. Kobayashi, T. and Shockey, D. A, Advanced Materials and Processes, Vol. 140-5 (1991) p. 28.
4. Kobayashi, T. and Shockey, D. A, Advanced Materials and Processes, Vol. 140-6 (1991) p. 24.
5. Edsinger, K., PhD Thesis - Department of Chemical and Nuclear Engineering, University of California, Santa Barbara (1995).
6. Edsinger, K., Odette, G. R., Lucas, G. E., Proceedings of the IEA International Symposium on Miniaturized Specimens for Testing Irradiated Materials, KFA Julich, September 22-23, 1994 (1995) p. 150.
7. Odette, G. R., Journal of Nuclear Materials, Vols. 212-215 (1994) p. 45.